Crystallization in heat-treated fluorochlorozirconate glasses

2009 J. Phys.: Condens. Matter 21 375103

(http://iopscience.iop.org/0953-8984/21/37/375103)

J. Phys.: Condens. Matter **21** (2009) 375103 (6pp) doi:10.1088/0953-8984/21/37/375103

Crystallization in heat-treated fluorochlorozirconate glasses

J A Johnson[1,6], J K R Weber[2], A I Kolesnikov[3] and S Schweizer[4,5]

[1] University of Tennessee Space Institute, Tullahoma, TN 37388, USA
[2] Materials Development, Incorporated, 820 Davis Street, Suite 129, Evanston, IL 60201, USA
[3] Neutron Scattering Sciences Division, Oak Ridge National Laboratory, Oak Ridge, TN 37831, USA
[4] Fraunhofer Center for Silicon Photovoltaics, Walter-Hülse-Straße 1, 06120 Halle (Saale), Germany
[5] Institute of Physics, Martin Luther University of Halle-Wittenberg, Heinrich-Damerow-Straße 4, 06120 Halle (Saale), Germany

E-mail: jjohnson@utsi.edu

Received 4 June 2009, in final form 25 July 2009
Published 11 August 2009
Online at stacks.iop.org/JPhysCM/21/375103

Abstract
Crystallization phenomena of fluorochlorozirconate glasses were investigated by means of differential scanning calorimetry and inelastic neutron scattering. The precipitation of barium chloride nanoparticles from the glass matrix upon heat treatment was found to be suppressed when re-melting the glass with a reducing agent but not if the agent was present in the initial synthesis. Addition of small amounts of oxide to the predominantly fluoride melt was found to maintain the presence of nanoparticles but not to induce the predicted phase transition of the barium chloride nanoparticles from hexagonal to orthorhombic structure. Inelastic neutron scattering performed on an 'as-made' glass and a heat-treated glass showed an increase in 'hardness', consistent with a more ordered structure.

1. Introduction

A fluorochlorozirconate glass based on a modified form of ZBLAN (comprised of zirconium, barium, lanthanum, aluminum, and sodium fluorides) is being developed as a glass ceramic for use in computed x-ray imaging systems. The materials are sensitive to ionizing radiation and can provide superior resolution to competing materials as they are optically transparent. They are made from Eu^{2+}-doped fluorochlorozirconate glasses that are heat-treated to nucleate europium-doped barium chloride nanocrystals, which sensitize the glass to ionizing radiation. Glass ceramics offer a combination of useful optical properties and the potential for near net shape fabrication of planar and shaped detectors [1–3]. The base glasses are well known since their discovery by Poulain *et al* [4]. They have low phonon energies and are used in infrared optics and devices. ZBLAN has a relatively low melting point of ≈750 °C and a glass transition temperature (T_g) of ≈230 °C [5].

Schweizer *et al* [6, 7] demonstrated that the temperature at which glasses are heat-treated influences phase selection during crystallization. At lower temperatures, ≈260 °C, Eu^{2+}-doped hexagonal barium chloride is formed; at higher temperatures, ≈290 °C, heat treatment leads to formation of orthorhombic barium chloride.

The precipitation of the barium chloride nanoparticles with respect to heat-treatment temperature and sample composition is the subject of this paper.

2. Experiment

2.1. Samples

Glass precursors were prepared from mixtures of high purity metal fluorides and chlorides (Sigma-Aldrich, Milwaukee, WI) that were handled in an inert-atmosphere glove box. The weighed halide powders were mixed together and placed in a platinum crucible with a close fitting lid. The crucible was heated in a horizontal tube furnace that was connected to one end of the glove box. The furnace cavity was made from a length of 100 mm inside diameter alumina tube sealed with a gasket at each end. After processing, the melt was poured into a brass mold held at a temperature of 200 °C. Glass samples were produced by casting 10 g batches that were

[6] Author to whom any correspondence should be addressed.

Table 1. Sample compositions in mol%.

Sample no.	Base composition							Dopant			
	ZrF_4	BaF_2	$BaCl_2$	NaCl	AlF_3	LaF_3	InF_3	EuF_2	$EuCl_2$	BaO_2	ABF
1	53	10	10	20	3	3.5	0.5	—	—	—	—
2	51	10	10	20	3	3.5	0.5	—	2	—	—
3	51	10	10	20	3	3.5	0.5	2	—	—	—
4	51	10	10	20	3	3.5	0.5	2	—	—	2
5[a]	51	10	10	20	3	3.5	0.5	2	—	—	—
6[b]	51	10	10	20	3	3.5	0.5	2	—	—	2
7	51	10	9.5	20	3	3.5	0.5	2	—	0.5	—

[a] Re-melt of sample #3.
[b] Re-melt of sample #5 with ABF.

melted at a temperature of 750 °C in a dry, inert atmosphere. The introduction of the molten glass into the mold resulted in a temperature rise of approximately 15 °C. The resulting material was cooled to room temperature in the mold at a rate of approximately 75 °C h^{-1}.

The sample compositions given in table 1 were investigated. Indium fluoride was used to stabilize ZrF_4 that is prone to reduce to ZrF_3. Ammonium bifluoride (ABF) was added to some batches. This provides a source of fluorine when it thermally decomposes to form nitrogen and hydrogen fluoride. Metal chlorides were substituted for some of the fluorides to enable precipitation of barium chloride nanocrystals during the heat-treatment step [2, 3, 6, 7]. The optical activity was induced by the addition of a europium(II) halide. Subsequent thermal treatment resulted in formation of the glass-ceramic product in which the optically active centers were dispersed in a transparent glass matrix. All the glasses investigated in this work were made with reagents from the same source and processed in platinum crucibles. Some prior work [3, 7] was performed using samples that were melted in glassy carbon crucibles. The use of a carbon crucible establishes reducing conditions in the high temperature melt which results in differences in the crystallization behavior of the two types of samples. These differences mainly relate to the exotherm temperatures that are attributed to differences in oxidation states that result from processing the melt in a carbon crucible.

2.2. *Differential scanning calorimetry and photoluminescence*

Differential scanning calorimetry (DSC) was used to determine the glass transition and crystallization temperatures of glasses. The DSC measurements were made using a Netzsch Maia DSC 200 F3 instrument. Glass samples weighing approximately 15 mg were loaded into sealed aluminum crucibles and heated at a rate of 10 °C min^{-1} to a maximum temperature of 450 °C. The DSC shows characteristic features of the thermal response, i.e. the glass transition temperature, T_g, an exotherm onset associated with nucleation of nanocrystalline barium chloride, and an exotherm onset associated with bulk crystallization. Additional higher temperature exotherms are attributed to reactions between crystalline phases and crystal consolidation. Results of these measurements were used to develop heat-treatment methods that grow the active phases pertaining to light output.

Photoluminescence spectra were taken with a Horiba Jobin Yvon FluoroLog-3 Spectrofluorometer. The excitation was provided by a xenon lamp set at 280 nm. An edge filter of 370 nm was engaged to avoid seeing the second harmonic of the excitation wavelength in the emission spectrum.

2.3. *Inelastic neutron scattering*

The inelastic neutron scattering (INS) spectra of as-quenched and heat-treated amorphous ZBLAN samples were measured on the low resolution medium energy chopper spectrometer (LRMECS) at the Intense Pulsed Neutron Source (IPNS) at Argonne National Laboratory (ANL) [8]. The spectrometer is a direct geometry machine: the incoming neutrons have a fixed energy E_i, selected by a rotating chopper, and the energy analysis is made on scattered time-of-flight neutrons. LRMECS has continuous detector coverage with scattering angles from 3° to 117° so that a broad range of wavevector transfers, Q, are measured simultaneously, e.g., 2 $Å^{-1} \leqslant Q \leqslant$ 12 $Å^{-1}$ at an energy transfer, $E = 25$ meV. This is extremely important in accurate determinations of the vibrational density of states, $G(\omega)$, when the neutron scattering is predominantly coherent, as it is in ZBLAN, which in the present study has the composition of sample 1, in table 1. The coherent (incoherent) neutron scattering cross sections (in barns) for the constituting atoms are: Ba – 3.23 (0.15), Cl – 11.53 (5.3), F – 4.02 (0.00), Zr – 6.44 (0.02), Na – 1.66 (1.62), Al – 1.50 (0.01), La – 8.53 (1.13), In – 2.08 (0.54) [9]. Unless the scattering is purely incoherent, it is necessary to average the measured neutron scattering over a large volume of reciprocal space in order for the resulting measurements to reflect the true vibrational density of states. INS experiments were carried out for about 40 h/sample at low temperature, $T = 10$ K, to reduce the multiphonon contribution and effect of the Debye–Waller factor. The data were also collected for an empty cell under similar conditions, for later subtraction from the sample data. The measurements were done with neutron incident energies $E_i = 35$ and 110 meV. The energy resolution of LRMECS is $\Delta E/E_i \approx$ 4–6% in the range of interest.

The theory of inelastic neutron scattering can be found in [10]. In the incoherent approximation, the scattering function is related to the generalized vibrational density of

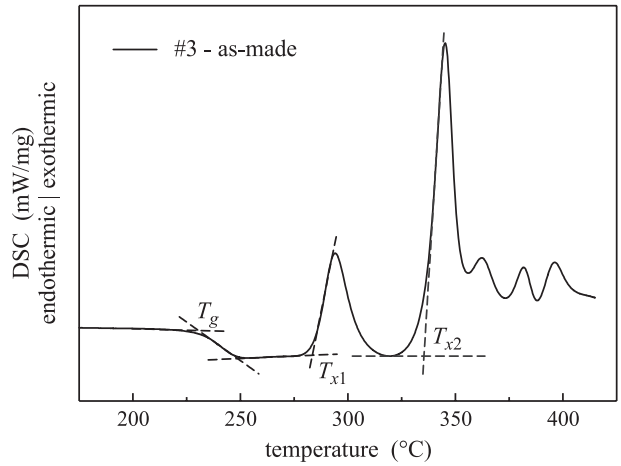

Figure 1. DSC results for a representative ZBLAN composition glass sample (sample #3). T_g is the glass transition temperature, T_{x1} and T_{x2} mark the onset temperature of the crystallization exotherms.

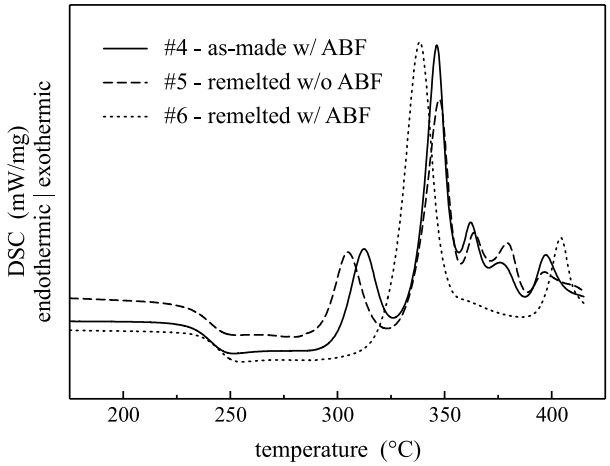

Figure 2. DSC of modifications to sample #3. Solid curve: sample #4 – 2 mol% of ABF included in initial synthesis, dashed curve: sample #5 (i.e. sample #3 re-melted), dotted curve: sample #6 (i.e. sample #5 re-melted with 2 mol% ABF).

states, $G(\omega)$, via

$$S(Q,\omega) = \frac{\hbar Q^2}{2m} e^{-2\bar{W}} \frac{[1+n(\omega,T)]}{\omega} G(\omega) \qquad (1)$$

where $S(Q,\omega)$ is the scattering dynamical structure factor, $\hbar Q$ is the neutron momentum transfer, $\hbar\omega$ is the energy transfer, $n(\omega,T) = [\exp(\hbar\omega/k_B T)-1]^{-1}$ is the population Bose factor for a mode of frequency ω, m is the atomic mass unit, and $e^{-2\bar{W}}$ is the effective (weighted averaged) Debye–Waller factor. The $G(\omega)$ function can be easily obtained from the above expression and represents the density of vibrational states weighted by the squared amplitude of the atomic displacements in the corresponding vibrational modes ω_λ and summed over all atoms:

$$G(\omega) = \sum_i \frac{f_i \sigma_i^{\text{tot}}}{3m_i} \sum_\lambda |e(i|\lambda)|^2 \delta(\omega-\omega_i) \qquad (2)$$

where $e(i|\lambda)$ is the eigenvector of the corresponding vibrational mode ω_λ, while m_i, σ_i^{tot} and f_i are the mass, total neutron scattering cross-section, and concentration of atom i. Thus, the contribution of different atoms in the measured INS spectrum is proportional to $\frac{f_i\sigma_i^{\text{tot}}}{3m_i}$ and this value is 65.2% for F, 25.3% for Cl, 4.6% for Zr, 3.6% for Na, and 1.3% for the rest of the atoms in the studied sample. Hence, the predominant contributions to the INS spectra for the studied ZBLAN sample are from neutron scattering on F and Cl atoms.

3. Results and discussion

3.1. Differential scanning calorimetry and photoluminescence

Figure 1 shows a representative DSC result obtained for the undoped ZBLAN composition. The addition of the europium(II) as either fluoride or chloride does not measurably alter the glass transition temperature, the precipitation onset of barium chloride nanoparticles or the onset of the crystallization of the glass matrix. These thermal events occur at approximately 230, 280, and 330 °C, respectively. In some samples, the effect of adding ABF was examined with respect to the formation of barium chloride nanocrystals as this is thought to maintain europium in the desired divalent state for maximizing light output. The DSC results shown in figure 2 indicate that when ABF is added to the mixture prior to initial melting, nanoparticles can be precipitated by heat treatment. If ABF is added to a crushed glass and re-melted, nanocrystals do not form during heat treatment, and the first exotherm at approximately 280 °C is absent. However, if the glass is re-melted without the additional ABF to the re-melt mixture, nanoparticles can be formed by heat treatment. Taken together, these results suggest that addition of ABF helps to stabilize the desirable oxidation states only if it is added during the first melting step. When ABF is added to a sample that has been melted before, it appears to 'strip' the chlorine from the melt leading to a composition that does not produce the nanophase particles when it is heat treated.

The result of a DSC experiment performed to illustrate the disappearance of the barium chloride nanoparticle precipitation is presented in figure 3. In this particular experiment an as-made glass of mass ≈20 mg is put into an aluminum crucible and loaded into the DSC. The sample is then heated to 310 °C and held there for 10 min; this temperature was chosen as figure 1 shows that the nanoparticle precipitation is complete at this temperature. After holding at 310 °C the sample is then cooled to 150 °C and held for another 10 min to come to equilibrium. Subsequently the sample is heated to 450 °C. The as-made glass exhibited an exotherm at a temperature of approximately 290 °C; the glass transition temperature is at 227 °C. During the second cycle of heat treatment the peak at 290 °C is absent and the glass transition is shifted to 252 °C which is typical for a ZBLAN base glass. The disappearance of the $BaCl_2$ crystallization peak after heat treatment has also been described in [7]. The crystallization exotherms at higher temperatures are similar to those already presented in figures 1 and 2.

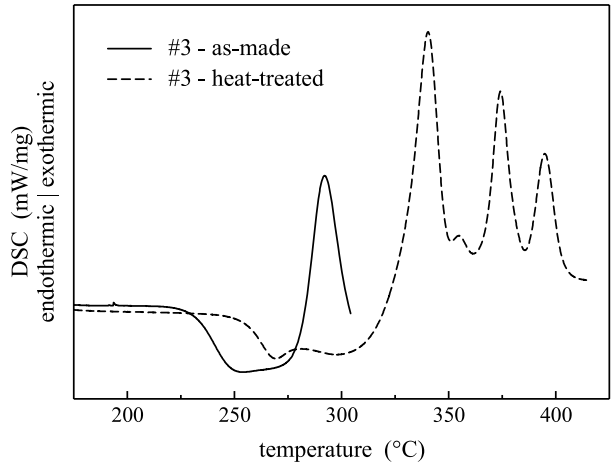

Figure 3. DSC scans of material from the same batch of glass. The as-made glass (solid curve) exhibits an exotherm centered at 260 °C that is absent in the spectrum from the heat-treated glass (dashed curve). The magnitude of glass transition is also diminished due to the heat treatment.

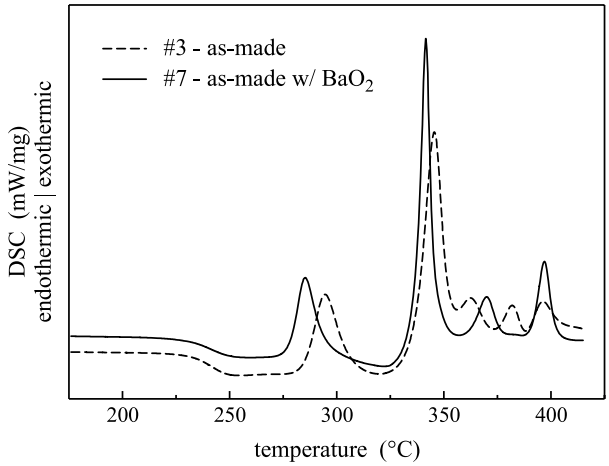

Figure 4. DSC results for a representative ZBLAN composition glass sample (sample #3) and a modification to sample #3 (sample #7). Solid curve: sample #7 – 0.5 mol% of BaO_2 included in initial synthesis and dashed curve: sample #3.

One important practical objective of the materials research is to increase the storage phosphor efficiency of the material [3]. In [1] and references therein it has been shown that oxygen plays a crucial role in the storage and read-out mechanism of storage phosphors. For example in the commercially-used x-ray storage phosphor BaFBr doped with divalent europium, divalent oxygen ions can substitute for fluorine and bromine; the halide vacancies necessary for charge compensation act then as additional electron trap centers resulting in an increased storage phosphor efficiency. In [11] it has been speculated that oxygen might be a trigger for the phase transformation from hexagonal to orthorhombic phase barium chloride in fluorochlorozirconate glass ceramics. Note, that the orthorhombic phase is responsible for the storage phosphor properties of these systems while the hexagonal phase is useful for scintillation applications. Thus, addition of small quantities of oxygen to the glass can on one hand trigger the phase transformation and on the other hand provide defects for efficient storage properties.

Traces of oxygen were introduced by adding small amounts of barium peroxide to the melt batch. Substitution of 0.5 mol% barium peroxide for barium chloride resulted in glasses that formed nanoparticles when they were heat treated as shown by the DSC trace in figure 4. It is also interesting to note that while T_g remains almost at the same position as in samples without barium peroxide the onset indicating the precipitation of barium chloride nanocrystals is shifted down by 10 to 270 °C.

Figure 5 shows photoluminescence spectra of samples #3 and #7; these are typical of hexagonal phase barium chloride [6, 7]. Therefore, although the 485 nm peak is diminished with the addition of barium peroxide, it did not trigger the phase transition to orthorhombic phase barium chloride even though the heat treatments at 310 °C were well above the temperature of formation for the nanocrystals, especially for the oxide-containing material. Studies are ongoing to enhance the oxygen defects by other methods.

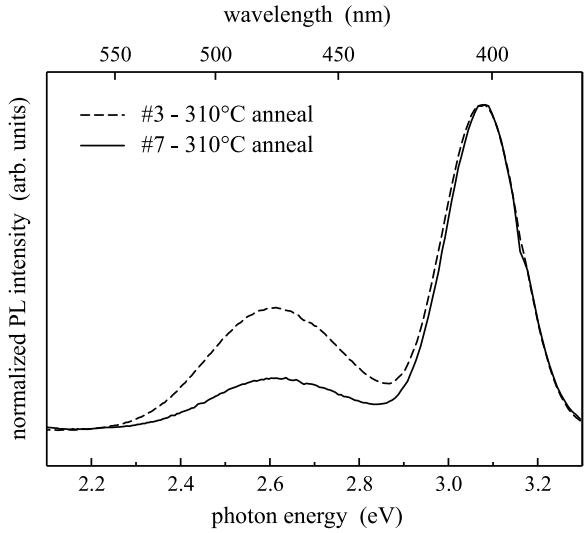

Figure 5. Normalized photoluminescence of spectra of Eu-doped FCZ samples #3 (dashed curve) and #7 (solid curve), both annealed at 310 °C for 10 min. The photoluminescence was excited at 280 nm.

3.2. Inelastic neutron scattering

Inelastic neutron scattering (INS) measurements had to be done on an undoped base glass (sample #1, table 1) as europium has a very large absorption cross-section. Experiments were performed on one as-made sample and one sample heat treated to the extent of full crystallization; substantial differences are seen in the spectra. In amorphous materials such as the one we are studying here the different bonding environments gives rise to vibrations over a wide range of frequencies. Results are shown in figures 6 and 7 for the spectra obtained with $E_i = 110$ and 35 meV, respectively. There is a small increase in intensity of the optical phonons in the high energy range around 90 meV for the heat-treated sample and a strong intensity redistribution at low energies. The as-made glass has a larger intensity for

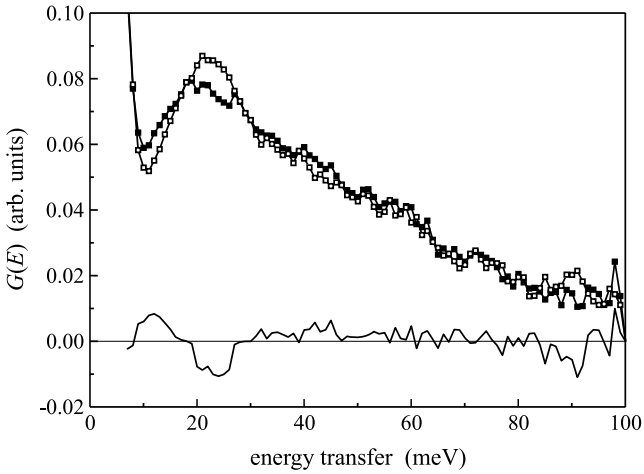

Figure 6. $G(E)$ spectra obtained from INS measurements for as-made and heat-treated glasses with $E_i = 100$ meV at $T = 10$ K; as-made sample (full squares), heat-treated sample (open squares), and difference spectrum (solid curve).

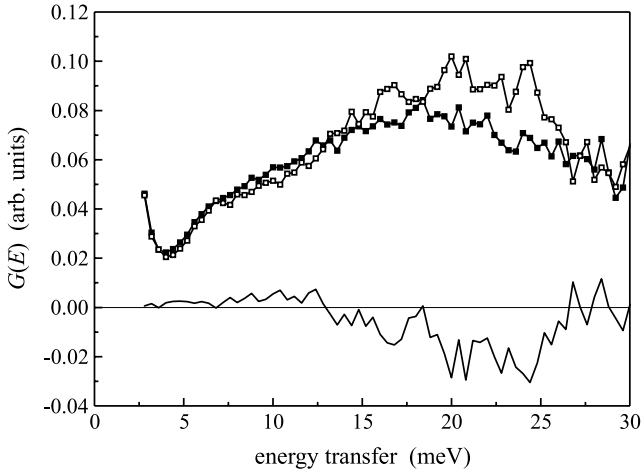

Figure 7. $G(E)$ spectra obtained from INS measurements for as-made and heat-treated glasses with $E_i = 35$ meV at $T = 10$ K; as-made sample (full squares), heat-treated sample (open squares), and difference spectrum (solid curve).

$E < 15$ meV, and between 30 and 70 meV, and lower intensity in the energy range 15–27 meV. The $G(E)$ spectra were corrected for an effective Debye–Waller factor $\exp(-\langle u^2 Q^2\rangle)$, which was obtained by fitting the $S(Q, E)$ spectra at energies around 25 meV with the formula

$$S(Q, E) = (aQ^2 + bQ^4)\mathrm{e}^{-\langle u^2 Q^2\rangle} \tag{3}$$

where a, b and $\langle u^2\rangle$ were the fitting parameters.

The aQ^2 and bQ^4 factors characterized the one-and two phonon scattering contributions, respectively. The result shows that the one phonon contribution is dominant; the effective mean-squared displacement, $\langle u^2\rangle \approx 0.005$ Å^2, obtained for both sample states, was used in the data treatment. The overall density of vibrational states obtained from the INS data are shown in the figure 8. They are almost featureless, even for the annealed (crystalline) sample. Only a few small peaks are seen

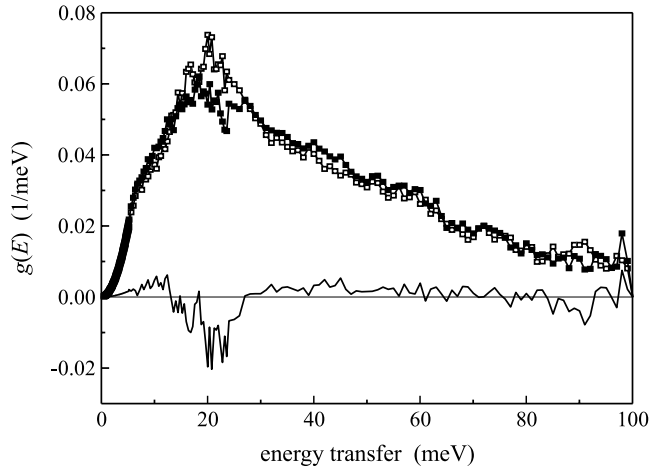

Figure 8. Density of vibrational states for as-made (full squares) and heat-treated (open squares) ZBLAN samples obtained from INS spectra, the low energy part, $E < 4$ meV is approximated by the Debye law, $g(E) \propto E^2$. The difference function (solid curve) is plotted.

around 20 meV, in the range where there is a large (≈15%) increase in the intensity for the annealed sample. Based on the data obtained the estimated heat capacity of the as-made sample compared to the annealed one should be larger at low temperatures and smaller at temperatures above ≈75 K.

4. Conclusion

The results of heat treatment show that DSC provides a convenient method to screen as-made glasses to predict their potential performance as x-ray sensor materials. In combination with optical measurements, the DSC is a convenient tool for glass development since it is a simple test to determine if the glass will produce the nanophase storage phosphor when it is heat treated.

Inelastic neutron scattering measurements are sensitive to the differences between as-made and heat-treated glasses and show softer behavior for the as-made glass. Thus, annealing results in more rigid properties of the glass, likely due to a higher degree of order in the sample.

Challenges that remain in the optimization of the glasses are in controlling the oxidation states of the components, particularly maintaining Zr^{4+} and Eu^{2+} states, which are both unstable in comparison to their respective trivalent state, and optimization of the heat-treatment protocols to maximize the concentration and distribution of nanoparticles for maximum light output. We have performed SEM [12] and TEM studies [6, 7] but feel that *in situ* heat-treatment TEM will give more insight into the growth kinetics. These measurements are ongoing along with synthesis of samples with different oxide doping.

Acknowledgments

This publication was supported by Grant Number 1R01EB006145-01A2 from the National Institutes of Health

(NIH) to the University of Tennessee Space Institute (UTSI) and under subcontracts from UTSI. Its contents are solely the responsibility of the authors and do not necessarily represent the official views of NIH. One of us (AIK) wishes to acknowledge ORNL/SNS which is managed by UT-Battelle, LLC, for the US Department of Energy under contract DE-AC05-00OR22725. We thank Mr Alexander Terekhov for his help in setting up and operating the glove box furnace system. S Schweizer was supported by the FhG Internal Programs under Grant No. Attract 692 034. Use of the Center for Nanoscale Materials was supported by the US Department of Energy, Office of Science, Office of Basic Energy Sciences, under Contract No. DE-AC02-06CH11357.

References

[1] Schweizer S 2001 Physics and current understanding of x-ray storage phosphors *Phys. Status Solidi* a **187** 335–93
[2] Johnson J A, Schweizer S, Henke B, Chen G, Woodford J, Newman P J and MacFarlane D R 2006 Eu-activated fluorochlorozirconate glass-ceramic scintillators *J. Appl. Phys.* **100** 034701
[3] Johnson J A, Schweizer S and Lubinsky A R 2007 A glass-ceramic plate for mammography *J. Am. Ceram. Soc.* **90** 693–8
[4] Poulain M 1983 Halide glasses *J. Non-Cryst. Solids* **56** 1–14
[5] Aggarwal I D and Lu G 1991 *Fluoride Glass Fiber Optics* ed I D Aggarwal and G Lu (New York: Academic)
[6] Schweizer S, Hobbs L W, Secu M, Spaeth J M, Edgar A and Williams G V M 2003 Photostimulated luminescence in Eu-doped fluorochlorozirconate glass ceramics *Appl. Phys. Lett.* **83** 449–51
[7] Schweizer S, Hobbs L W, Secu M, Spaeth J M, Edgar A, Williams G V M and Hamlin J 2005 Photostimulated luminescence from fluorochlorozirconate glass ceramics and the effect of crystallite size *J. Appl. Phys.* **97** 083522
[8] http://www.pns.anl.gov/instruments/lrmecs/
[9] Sears V F 1992 Neutron scattering lengths and cross sections *Neutron News* **3** 26–7
[10] Axe J D 1976 *Physics of Structurally Disordered Materials* ed S S Mitra (New York: Plenum)
[11] Chen G, Johnson J, Woodford J and Schweizer S 2006 Insights into phase formation in fluorochlorozirconate glass-ceramic storage phosphors *Appl. Phys. Lett.* **88** 191915
[12] Chen G, Johnson J, Weber R, Nishikawa R, Schweizer S, Newman P and MacFarlane D 2006 Fluorozirconate-based nano glass ceramics for high-resolution medical x-ray imaging *J. Non-Cryst. Solids* **352** 610–4